*IOSR Journal of Applied Chemistry (IOSR-JAC)*
*e-ISSN: 2278-5736.Volume 16, Issue 1 Ser. II (January 2023), PP 01-10*
*www.iosrjournals.org*

# Sulphonated Ti-MCM41: A Potential Catalyst for the Transformation of Bio-Glycerol to Solketal

Balakrishna Matkala,[1,2] Sasikumar Boggala[3], Yadaiah Salwadi[1], Hari Padmasri Aytam[1*]

[1]*Department of Chemistry, Osmania University, Hyderabad-500 007, Telangana, India.*
[2]*Department of Chemistry, SR & BGNR Govt. Arts & Science College (A), Khammam, Telangana, India.*
[3]*Catalysis & Fine Chemicals Department, CSIR-Indian Institute of Chemical Technology, Hyderabad-500 007, Telangana, India.*
**For Correspondence: ahpadmasri@gmail.com; ahpadmasri@osmania.ac.in*

***Abstract***
*MCM-41 supported Titanium catalyst (Si/Ti =150) and sulphate modified titanium catalysts were synthesized by sol-gel process. The potential of these catalysts was determined by acetalization reaction to produce solketal from glycerol. To understand the effect of sulphonation in this catalytic process, 1N $H_2SO_4$ was impregnated on the surface of the Ti-MCM-41. The incorporation of Ti into the frame work of MCM-41 was authenticated by Fourier transformed IR spectroscopy, X-ray diffraction and $N_2$ -sorption studies reveal the existence of mesoporous structure and uni-dimensional pores. $NH_3$-TPD results showed the generation of Lewis acid sites, which are due to incorporation of titanium (IV) into the silica frame work. Upon sulphonation the acidity on the surface of the catalysts increases and facilitates the conversion of glycerol.*

***Key words*****:** *Glycerol, Sulphate modified Ti-MCM-41, sol-gel process, Acidity and Solketal.*

---

Date of Submission: 05-01-2023 Date of Acceptance: 19-01-2023

---

## I. INTRODUCTION

Bio-diesel is an alternative fuel produced by transesterification of inedible oils and it is compatible with commercial diesel engines [1]. In the view of environmental concerns the usage of bio-diesel rapidly increases year by year. During the production of bio-diesel, glycerol is obtained as a main by-product. It is about that 10wt% of the crude glycerol generated of total biodiesel production [2].The cost of the bio-diesel production process is decided by the utilization of main by product, glycerol. In this regard, there are many reports to transform this crude glycerol to value added chemicals and fuel additives [3-4]. In this present work mesoporous molecular sieves namely MCM-41 are used as catalyst support for the transformation of glycerol into solketal. Solketal is fuel additive and it has several other applications in polymer, cosmetics and pharmaceutical industry. MCM-41 possesses adequate surface area, pore volume and good thermal stability. With these attractive properties MCM-41 has a lot of applications; one of its important applications is used in heterogeneous catalysis and also used in pharmaceutical industry, environmental protection [5-8]. The incorporation of heteroatoms into silica frame work (like Al, Ti, Zr, Cr, V etc) of MCM-41, a significant increase in acidity is observed [9] and facilitate the generation of more number of active sites over the catalyst, which improves the catalytic activity [10-12]. In the present study titanium is incorporated into the frame work of MCM-41 during the synthesis by sol-gel method. It leads to the generation of weak Lewis and Bronsted acid sites over the catalyst. By impregnating the sulphate groups on Ti-MCM-41 results in considerable changes in the acidity over the catalyst and improves the catalytic activity drastically towards the conversion of glycerol to solketal (Scheme 1).

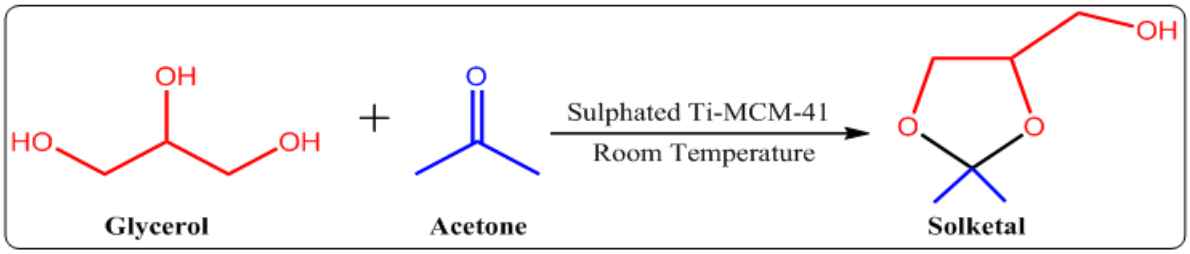


**Scheme 1: Glycerol acetalization over sulphated Ti-MCM-41**

## II. EXPERIMENTAL SECTION

### *2.1 Chemicals*

Cetyl trimethyl Ammonium bromide (CTAB), Tetraethyl orthosilicate (TEOS), Titanium isopropoxide ($Ti(OiPr)_4$), 25% Aqueous $NH_4OH$ solution and $H_2SO_4$ are of Sigma-Aldrich make, AR grade and used in the preparation of present catalysts.

### *2.2 Preparation of Ti-MCM-41 and sulphate modified Ti-MCM-41*

The titanium containing mesoporous catalyst (Si/Ti=150) was prepared by sol-gel method. TEOS (Tetra ethyl orthosilicate), TTIP (titanium tetra isopropoxide or titanium isopropoxide) were used as silica and titanium sources respectively. CTAB (Cetyltrimethyl ammonium bromide) was used as surfactant. Firstly, CTAB was dissolved in water and 25% of ammonium hydroxide added to this solution, mixed thoroughly by vigorous stirring. After that silica and titanium precursors were added to this solution. The resultant solution mixture was stirred at room temperature 300-400 rpm for 3hours. The sample was separated by filtration and washed with deionized water thoroughly, dried at 100$^{o}$C for overnight. Finally the obtained dried powder sample was calcined at 550$^{o}$C for 5 hours at a heating rate of 5$^{o}$C/min., is Ti-MCM-41.

To prepare the sulphate modified Ti-MCM-41catalyst, 1N $H_2SO_4$ was impregnated on 1gm of Ti-MCM-41 excess water was allowed to evaporate. Then the sample was kept in oven and dried over night at 100$^{o}$C. The dried powder was calcined in a muffle furnace at 550$^{o}$C for 5 hours at a heating rate of 5$^{o}$C/min. The obtained catalyst was denoted as S/Ti-MCM-41(Where "S" indicates the sulphonation).

### *2.3 Characterization studies*

The small and wide angle XRD analysis of the synthesized catalysts were conducted on a Rigaku Ultima-IV X-ray diffractometer using Ni filtered Cu Kα radiation (λ = 0.15418 nm) with a scan rate of $2^{o}$ $min^{-1}$ at 40KV and 20 mA. The $N_2$ adsorption-desorption were recorded at 77.3K on Autosorb iQ Station 1. Samples were degassed at 200$^{o}$C for 2hours, prior to the measurements. By using BET (Brunauer-Emmett-teller) equation specific surface area was calculated. The pore size distributions were calculated by the BJH (Barret-Joyner-Halenda) equation. The TG-DTA analysis was conducted on SDT Q600 V20.9 Build 20, room temperature to 800°C @ 20 °C/min $N_2$ Purge = 100 mL/min. The surface morphology of the synthesized catalysts were determined by SEM (Scanning Electron Microscopy) analysis using JEOL, JSM—6390LV, equipped with an Energy Dispersive X-ray Spectrometer (EDS). The XPS (X-ray photoelectron Spectroscopy) analysis was conducted using ESCA 3400 photoelectron spectrometer, using Mg $K_\alpha$ radiation of 1253.6 eV. The FT-IR spectra of synthesized catalysts were recorded in the range of 400-4000 $cm^{-1}$ on Thermo Nicolet iS50 with inbuilt ATR. The $NH_3$-TPD analysis was performed on an Auto Chem 2910 (Micromeritics).

### *2.4 Catalytic reaction*

The conversion of glycerol to solketal via acetalization reaction was conducted in a batch type glass reactor equipped with a septum and magnetic stirrer. First appropriate amounts of catalyst, glycerol and acetone were added into the reactor. Then the reaction mixture was magnetically stirred at room temperature. The reaction mixture was collected at regular time intervals from the reactor and analysed by a GC (Agilent 1020A-FID). This process was carried out with different wt. % of the synthesized catalysts (like 1/3/5 wt. %) and different mole ratios of glycerol and acetone (like 1:6/1:8 /1:10) till steady state was attained. After that catalyst was separated from the reaction mixture by centrifugation, washed with deionized water, dried in oven at 100 ºC overnight and examined for the recyclability. The glycerol conversion and solketal selectivity were calculated based on the following equations:

$$\text{Glycerol conversion (\%)} = \frac{(\text{Moles of glycerol})\text{initial} - (\text{Moles of glycerol})\text{final}}{(\text{Moles of glycerol})\text{initial}} \times 100$$

$$\text{Solketal selectivity (\%)} = \frac{\text{Moles of solketal formed}}{(\text{Moles of glycerol})\text{initial} - (\text{Moles of glycerol})\text{final}} \times 100$$

## III. RESULTS AND DISCUSSION

### *3.1 XRD analysis*

Figure 1A and 1B show the Low angle and wide angle XRD patterns of the Ti-MCM-41 and sulphate modified Ti-MCM-41. Figure 1A reveals both the synthesized catalysts show peak at around 2θ = 0.282 and $0.303^{o}$ that corresponds to the $d_{100}$ plane, characteristic peak of mesoporous materials (ICDD # 49–1712).The other two peaks indexed to the $d_{110}$ and $d_{200}$ planes respectively, shows the development of an organised mesoporous structure [13].Upon sulphonation the intensity of the peak ($d_{100}$) increases, even though the structure of the catalyst remains intact [14]. From Figure 1B, both the catalysts show a broad peak around 23$^{o}$ due to amorphous silica [15].There is no other peak observed in both the samples corresponding to titania,

probably due to high dispersion of titania on the surface of the silica frame work [15]. By using the formula $a_0 = 2d_{100}/\sqrt{3}$ unit cell parameter is calculated and presented in Table 1. From Table 1, d-spacing value and unit cell parameters of sulphonated Ti-MCM-41 show increased values this may be due to the extra frame work formation of $OSO_3H^-$-Ti-MCM-41.

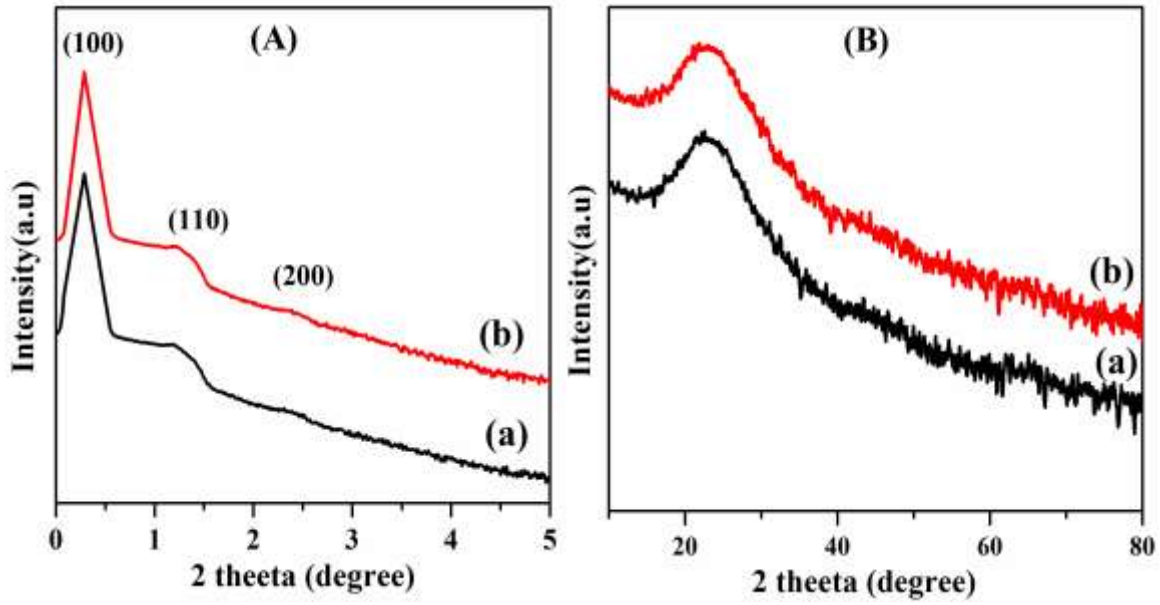


**Figure 1:** (A) Low and (B) Wide angle XRD Patterns of (a)Ti-MCM-41 and (b) S/Ti-MCM-4

### *3.2 BET adsorption isotherms and Pore size distribution*

The $N_2$ adsorption-desorption isotherms of the Ti-MCM-41 and S/Ti-MCM-41 are shown in Figure 2A. The resultant textural properties were presented in Table 1. From Figure 2A it can be observed that both the catalysts exhibits a type IV isotherm,classified by IUPAC.Which indicates the mesoporous nature of materials [16].The relative pressure($p/p^o$) at less the 0.4, $N_2$ was adsorbed(mono layer) on the pore walls of the both the samples. A significant modulation was noticed between the relative pressures of 0.4-0.8. This is a result of capilary condensation during the adsorption process and is a sign of the samples mesoporosity[15].The pore size distributions for both the samples are shown in Figure 2B. The average pore size and pore volume of Ti-MCM-41 are 1.868 nm and 0.346 cc/g respectively, observed. After impregnation of sulphate groups on Ti-MCM-41 the pore size (2.419 nm) and pore volume(0.479 cc/g) increases. This may be due to the widening of the mesopores by the sulphate groups. As shown in Table 1, the surface area increases even after the impregnation of sulphate groups into the frame work of Ti-MCM-41.This is may be due to the potential introduction and proper anchoring of $OSO_3H^-$ to Ti-MCM-41.

**Table 1:** ***Textural properties of the Ti-MCM-41 and S/Ti-MCM-41***

| S. No. | Catalysts | BET Surface area [a] ($m^2/g$) | Pore volume [a] (cc/g) | Pore diameter [a] (nm | d-spacing [b] (nm) $\times10^{-4}$ | Unit cell parameter [b] ($a_o$) (nm) $\times10^{-4}$ | Total acidity [c] (µmol/g) |
|---|---|---|---|---|---|---|---|
| 1. | Ti-MCM-41 | 389.04 | 0.346 | 1.868 | 1.89 | 2.18 | 90 |
| 2. | S/Ti-MCM-41 | 523.47 | 0.479 | 2.419 | 2.03 | 2.34 | 118 |

*[a] from $N_2$ sorption studies; [b] from XRD-analysis; [c] from $NH_3$-TPD analysis.*

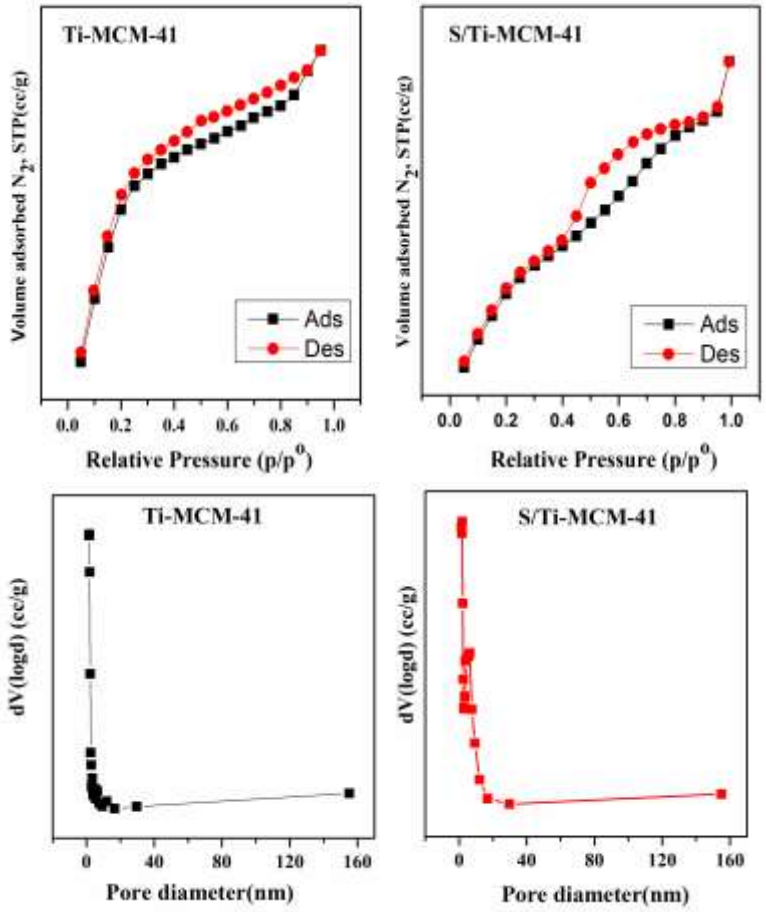


**Figure 2: BET isotherms and pore size distribution curves of Ti-MCM-41and S/Ti-MCM-41**

***3.3 TG-DTA analysis***

The thermal decomposition of the Ti-MCM-41 and S/Ti-MCM-41 was studied by using TG-DTA analysis and presented in Figure 3. It shows the two weight loss regions. The first weight loss region was noticed in the range of 50-150 $^{o}$ C, it is 23.53% for Ti-MCM-41 and for S/Ti-MCM-41 is18.02%. This can be assigned to the elimination of chemically bonded water molecules [16]. The second weight loss region was noticed in the range of 150-650$^{o}$ C, it is 6.4% for Ti-MCM-41 and 3.5% for S/Ti-MCM-41. This can be attributed to the decomposition and removal of organic template [17].

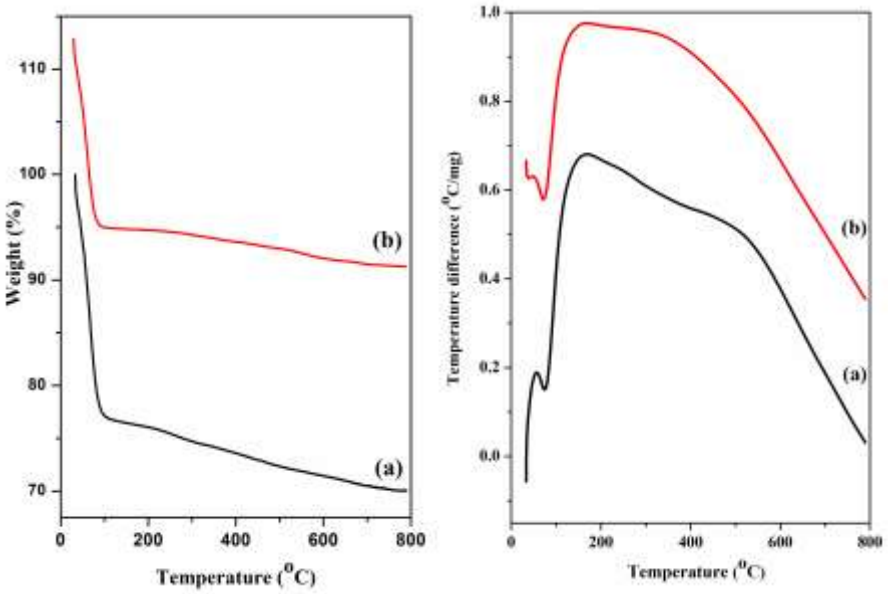


**Figure 3: TG-DTA curves of (a) Ti-MCM-41 and (b) S/Ti-MCM-41**

### *3.4 Scanning Electron Microscopy (SEM) analysis*

The Surface morphology of the samples was investigated by Scanning Electron Microscopy (SEM). Figure 4A and 4B show the SEM images and EDAX of Ti-MCM-41 and S/Ti-MCM-41 respectively. In both the samples the particles can be seen as spherical in shape. The particle size of Ti-MCM-41 varies from 304-490 nm, whereas in case of S/Ti-MCM-41 it is 273-474 nm. EDAX spectra show the presence of Si, Ti, C, O in both the samples and also S in S/Ti-MCM-41 which indicates the proper incorporation of Ti into the silica frame work and successful impregnation of sulphate groups on Ti-MCM-41.

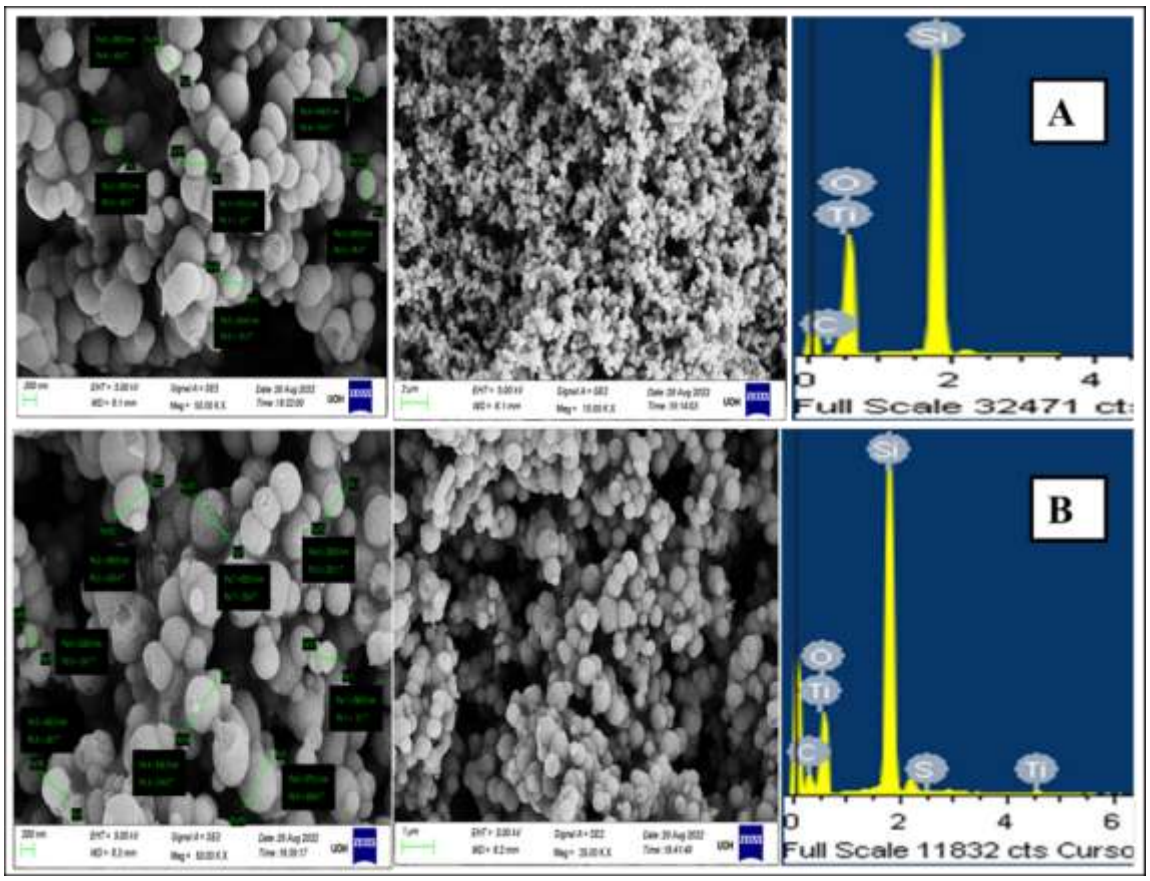


**Figure 4: SEM images and EDAX spectra of (A) Ti-MCM-41 and (B) S/Ti-MCM-41**

### *3.5 X-ray Photoelectron Spectroscopy (XPS)*

In order to determine the surface compositions, chemical and electronic states of atoms of the catalysts, XPS technique is recorded for the S/Ti-MCM-41 sample and shown in Figure 5. Figure 5A confirms the presence of $Si^{4+}$ in the Ti-MCM-41 frame work due to occurrence of Si $2p_{1/2}$ at around 107 eV (Si-O links in $SiO_4^{-4}$ units). Figure 5B shows the Ti 2p XPS spectrum consists of two peaks with binding energies 463.09 and 468.4 e V can be assigned to the Ti $2p_{3/2}$ and Ti $2p_{1/2}$ respectively. It confirms the existence of $Ti^{4+}$ ions in Ti-MCM-41[16, 18]. Figure 5C reveals the presence of S in the Ti-MCM-41 frame work due to the occurrence of S $2p_{1/2}$ at around 157.8 e V. This indicates the successful impregnation and proper anchoring of $OSO_3H^-$ to Ti-MCM-41. The spectrum (Figure 5D) shows a strong O 1s peak with binding energy 536.5eV, indicates that oxygen atoms are linked to silicon by Si-O connection [19]. These Si-O connections are Si-O-Si, Si-OH and Si-O-Ti.

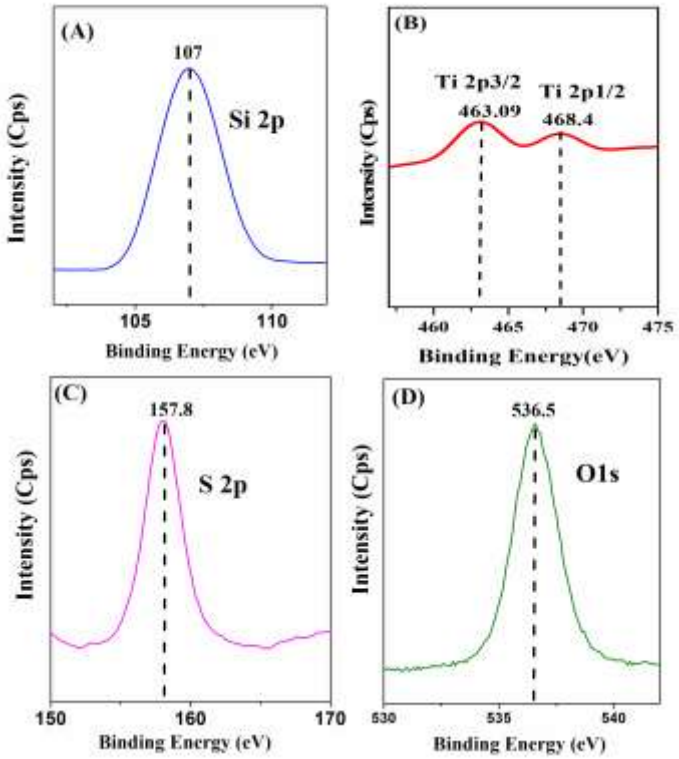


**Figure 5: XPS spectra of S/Ti-MCM-41 (A) Si 2p (B) Ti 2p (C) S 2p and (D) O 1s**

### *3.6 FTIR Spectroscopy*

Figure 6A&B displays the FT-IR results of Ti-MCM-41 and S/Ti-MCM-41 respectively. The peak observed in both the samples at 1640 $cm^{-1}$ corresponds to the presence of Si-OH group, is the main characteristic of mesoporous samples [15]. Ti-MCM-41 and S/Ti-MCM-41 catalysts show peaks at around 964.4 and 968.4 $cm^{-1}$ attributed to the presence of Si-O-Ti, this indicates incorporation of titanium and its existence in tetrahedral coordination within the silica frame work [16, 20]. The presence of Si-O-Ti in the mesoporous silica structure indicates that $Si^{4+}$ was replaced with $Ti^{4+}$. The incorporation of Ti into the silica frame work results in the generation of both Lewis and Bronsted acidity [21]. The major FTIR band appeared at 1072 $cm^{-1}$ can be assigned to the asymmetric stretching vibrations in the Si-O-Si linkage present in the silica frame work [22]. The band observed at around 453 $cm^{-1}$ is assigned to the bending vibration of the Si-O groups [23]. In S/Ti-MCM-41 a weak band observed at 883 $cm^{-1}$ correspond to the stretching vibration of the S=O group [24], which indicates the presence of $OSO_3H^-$ on the pore wall of the Ti-MCM-41. This may be attributed to increase in the acidity on surface of the sample.

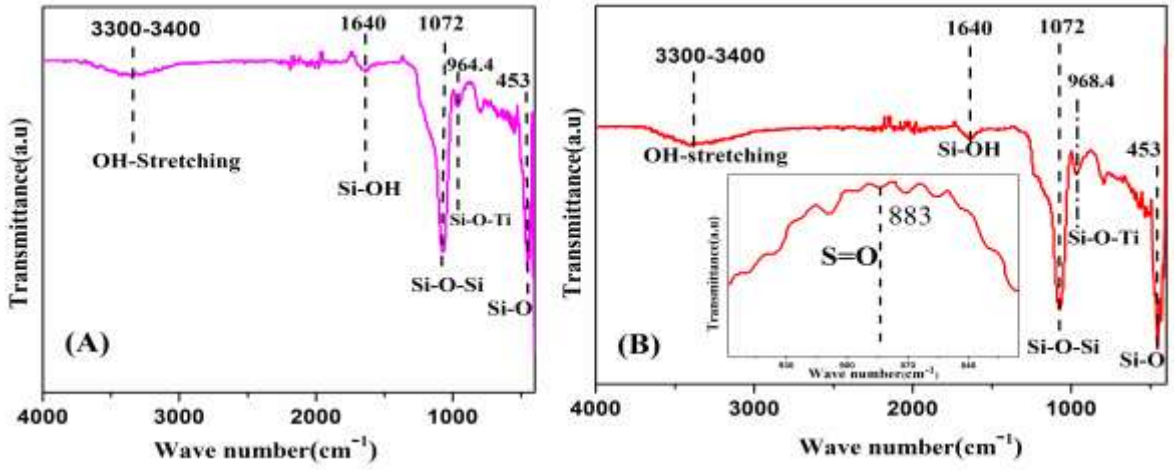


**Figure 6: FTIR spectrum of (A) Ti-MCM-41 and (B) S/Ti-MCM-41**

### *3.7 Temperature programmed desorption of Ammonia ($NH_3$-TPD)*

In order to determine the acidic strength of the Ti-MCM-41 and S/Ti-MCM-41, Temperature programmed desorption of ammonia was performed and the profiles were shown in Figure 7. The acid sites were distinguished as weak (less than 250 $^oC$), medium (250-450 $^oC$) and strong (above 450 $^o$ C) based on the ammonia desorption profiles. Ti-MCM-41 mostly shows the moderate Lewis and Bronsted acidity due the presence of $Ti^{4+}$and coordination of OH-group with the titanium respectively. Whereas sulphate modified Ti-MCM-41 samples shows weak, moderate and strong acid sites. After sulphonation $OSO_3H^-$ groups bind to the titanium frame work as $OSO_3H$-Ti-OH, generates more Bronsted acidity. The high intensity peak observed at 550 $^oC$ reveals the desorption of $NH_3$ molecules from tetrahedral titanium IV centre, it indicates that within the mesoporous framework the strong acid sites were tetrahedrally coordinating with the titanium centre[17].The total acidity values of both the samples were presented in Table 1, it indicates S/Ti-MCM-41 possess high acidity (118 µmol/g) than the Ti-MCM-41(90 µmol/g).These findings reveal that by impregnating the sulphate groups weak acid sites present on Ti-MCM-41 transform into the strong acid sites. Thus it may be concluded that sulphonation favours enhancement of the acidity of the catalyst and conversion of glycerol by acetalization reaction.

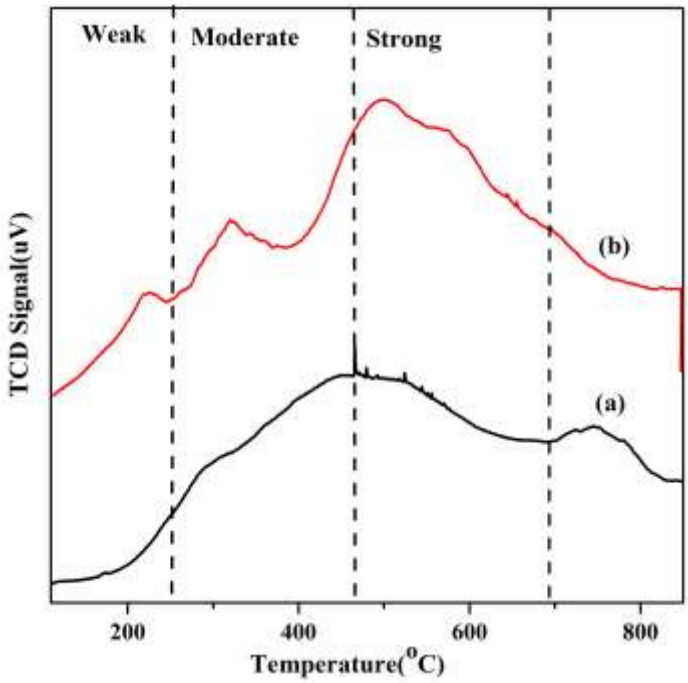


**Figure 7: $NH_3$ – TPD profiles of (a) Ti-MCM-41 and (b) S/Ti-MCM-41**

### *3.8 Activity Studies of Glycerol acetalization*

The Ti-MCM-41 and sulphate modified Ti-MCM-41(Si/Ti = 150) were used for glycerol acetalization reaction. As shown in Figure 8(A) and 8(B) Sulphate modified titanium sample(S/Ti-MCM-41) shows highest glycerol conversion of 91.98% as compared to the bare Ti-MCM-41(30.25%). Also the selectivity of solketal found to be 98% for S/Ti-MCM-41 and around 55% for bare Ti-MCM-41. The better activity of the S/Ti-MCM-41 is probably due to the generation of well dispersed strong acid sites over the catalyst that is authenticated by $NH_3$-TPD analysis (Figure 7). In addition to strong acid sites, S/Ti-MCM-41 possesses high surface area, pore volume and pore diameter than the bare Ti-MCM-41(shown in Table 1). These cooperative factors will enhance the catalytic activity. The optimized reaction parameters such are substrate molar ratios, catalyst weight percentages (of Ti-MCM-41 and S/Ti-MCM-41) and time on stream studies are taken into consideration. To optimize the substrate mole ratio the reaction was carried out by varying the mole ratios of glycerol to acetone as 1:6, 1:8 and 1:10 over S/Ti-MCM-41. With increasing the glycerol to solketal molar ratio from 1:6 to 1:10, the catalytic activity increases as shown in Figure 9A. Further increasing the molar ratio not much change was noticed in the catalytic activity. The role of catalyst weight percentage on catalytic activity is examined with 1wt%, 3wt% and 5wt% of the catalyst separately. With the increase in catalyst wt. % from 1 to 3, increase in glycerol conversion and selectivity to solketal was observed as shown in Figure 9B indicating the presence of

additional active sites to have enhanced the catalytic activity. Further increasing the catalyst wt. % from 3 to 5, there is no appreciable enhancement in the catalytic activity. The time on stream studies were also investigated for the catalytic activity. As reaction time increases from 30 to 120 min, glycerol conversion and solketal selectivity increases. At 120 min of reaction time, highest catalytic activity was obtained. Further increasing the reaction time to 150 min, no considerable improvement in catalytic activity could be seen. The reaction carried out at room temperature showed better catalytic activity; upon increasing the reaction temperature no change in the catalytic activity was observed.

From these investigations the optimal reaction conditions obtained were, catalyst**:** S/Ti-MCM-41, mole ratio of glycerol to solketal**:** 1:10, catalyst wt. %**:** 3, reaction time**:** 120 min and at room temperature. The recyclability studies of the S/Ti-MCM-41 reveal that, it retains its activity towards glycerol conversion up to 4 cycles (shown in Figure 10), indicates the reusability of S/Ti-MCM-41.

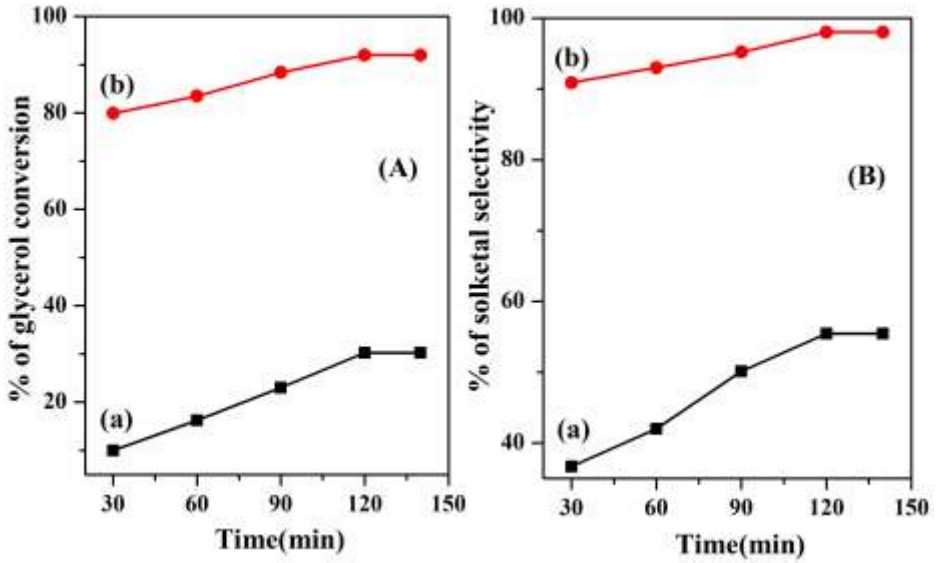


**Figure 8: (A) % Conversion of glycerol and (B) % selectivity of solketal v/s time of (a) Ti-MCM-41 and (b)S/Ti-MCM-41; over 3wt. % of the catalyst, glycerol: acetone mole ratio 1:10, at room temperature**

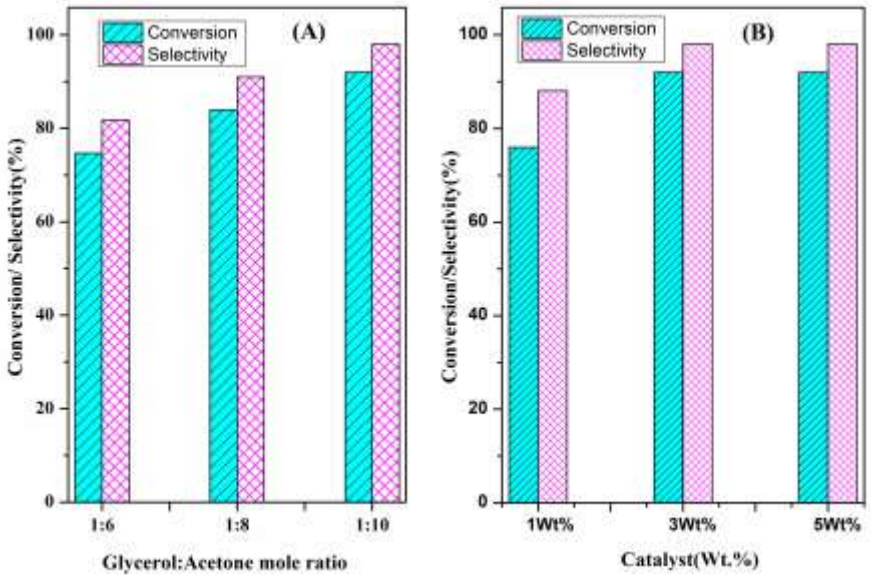


**Figure 9: Conversion of glycerol (%) and Selectivity of solketal (%) (A) at different substrate mole ratios and (B) at different wt. % of the catalyst S/Ti-MCM-41**

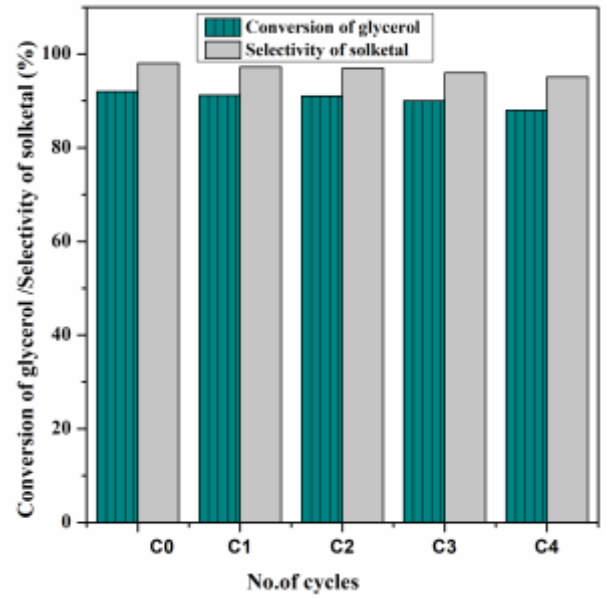


**Figure 10: Recycle studies of S/Ti-MCM-41, catalyst weight % : 3, glycerol: acetone : 1:10, time:120min, at room temperature**

## IV. CONCLUSIONS

In conclusion, titanium incorporated MCM-41 and sulphate modified Ti-MCM-41catalysts were synthesized by sol-gel and impregnation methods. These are characterized by various techniques and their catalytic activity was compared by conversion of glycerol into solketal at different reaction conditions. Our studies reveal that S/Ti-MCM-41 catalyst shows higher glycerol conversion (91.98%) and solketal selectivity (98.02%) than the bare Ti-MCM-41 at room temperature. The better efficiency of S/Ti-MCM-41 towards glycerol conversion was because of its adequate surface area, presence of strong acidic sites and compatible pore size. Also this catalyst retains it catalytic activity up to 4 cycles. Therefore, S/Ti-MCM-41 is a better and reusable solid acid catalyst used in the conversion of glycerol into solketal.

### CONFLICT OF INTEREST

Authors declare no conflict of interest.

### ACKNOWLEDGEMENTS

The authors thank Dr. A. Venugopal, Senior Principal Scientist, Catalysis & Fine Chemicals Division, CSIR-IICT for some of the characterization analysis of catalysts and GC analysis of the reaction samples.

### REFERENCES

[1]. M.A. Fazal, A.S.M.A. Haseeb, H.H. Masjuki. Biodiesel feasibility study: An evaluation of material compatibility; performance; emission and engine durability. Renewable and Sustainable Energy Reviews 2011; 15(2): 1314-1324.
[2]. D.T Johnson, K.A Taconi. The glycerin glut: options for the value-added conversion of crude glycerol resulting from biodiesel production Environ. Prog. 2007; 26: 338–348.
[3]. C.-H. (Clayton) Zhou, J.N. Beltramini, Y.-X. Fan, G.Q. (Max) Lu, Chem. Soc. Rev. 2008; 37: 527–549.
[4]. R. Sarkari, Ch. Anjaneyulu, V. Krishna, R. Kishore, M. Sudhakar, A. Venugopal, Catal. Commun. 2011; 12: 1067–1070.
[5]. T. Tatsumi, K. A. Koyano, N. Igarashi. Remarkable activity enhancement by trimethyl silylation in oxidation of alkenes and alkanes with $H_2O_2$ catalyzed by titanium-containing mesoporous molecular sieves. Chem. Commun.1998; (3): 325–326
[6]. F. Subhan, B. S Liu, Y. Zhang, G. Li X. High desulfurization characteristic of lanthanum loaded mesoporous MCM-41 sorbents for diesel fuel. Fuel Process. Technol.2012; 97: 71–78.
[7]. P.Selvam, S.K. Bhatia, C. G. Sonwane. Recent advances in processing and characterization of periodic mesoporous MCM-41 silicate molecular sieves. Ind. Eng. Chem. Res. 2001; 40(15): 3237–3261.
[8]. Y. Kong, H. Y. Zhu, G. Yang, X. F. Guo, W. H. Hou, Q. .J Yan, M.Gu, C. Hu. Investigation of the structure of MCM-41 samples with a high copper content. Adv. Funct. Mater. 2004; 14(8): 816– 820.
[9]. S.P. Naik, V Bui, T. Ryu, J D. Miller, W. Zmierczak. Al-MCM-41 as methanol dehydration catalyst. Appl. Catal. A: Gen. 2010; 381(1-2):183-190.
[10]. S. Wang, C. Ma, Y. Shi, X. Ma. Ti incorporation in MCM-41 mesoporous molecular sieves using hydrothermal synthesis. Front. Chem.Sci. Eng. 2014; 8(1):95-103.
[11]. E. Kraleva, M. L. Saladino, A. Spinella, G. Nasillo, E. Caponetti. $H_3PW_{12}O_{40}$ supported on mesoporous MCM- 41 and Al-MCM-41 materials: Preparation and characterisation. J.Mater. Sci. 2011; 46(22): 7114–7120.
[12]. Q. Luo, F. Deng, Z. Y. Yuan, J. Yang, M .J. Zhang, Y. Yue, C. H Ye. Using trimethylphosphine as a probe molecule to study the acid states in Al-MCM-41 materials by solid-state NMR spectroscopy. J Phys.Chem. B. 2003; 107(11): 2435–2442

[13]. M.S. Salam, M.A. Betiha, SA. Shaban, A.M. Elsabagh, .RM. Abd El-Aal. Synthesis and characterization of MCM-41-supported nano zirconia catalysts. Egypt. J. Pet. 2015; 24(1): 49-57.
[14]. K.M. Parida, D.Rath . Studies on MCM-41: Effect of sulfate on nitration of phenol. J. Mol. Catal. A: Chem. 2006; 258(1-2), 381-387.
[15]. R, Peng, D. Zhao, N.M. Dimitrijevic, T.Rajh, R.T. Koodali. Room temperature synthesis of Ti–MCM-48 and Ti–MCM-41 mesoporous materials and their performance on photo catalytic splitting of water. J. Phys. Chem. C. 2012; 116(1):1605-1613.
[16]. M.M. Ambursa, P. Sudarsanam, L.H. Voon, S.B. Abd Hamid, S.K. Bhargava. Bimetallic Cu-Ni catalysts supported on MCM-41 and Ti- MCM-41 porous materials for hydrodeoxygenation of lignin model compound into transportation fuels. Fuel Process.Technol.2017; 162: 87-97.
[17]. K.V. Wagh , A.L. Gajengi, D. Rath, K.M. Parida, BM. Bhanage. Sulphated Al-MCM-41: A simple, efficient and recyclable catalyst for synthesis of substituted aryl ketones/olefins via alcohols addition to alkynes and coupling with styrenes. Mol. Catal.2018; 452: 46-53
[18]. H. Chen, Y.-P. Peng , K.-F. Chen, C.-H. Lai,Y.-C. Lin, Rapid synthesis of Ti-MCM-41 by microwave- assisted hydrothermal method towards photo catalytic degradation of oxytetracycline. J. Environ. Sci.2016; 44 : 76–87.
[19]. J.C. Bedoya, R. Valdez, L. Cota, MA. Alvarez-Amparán, A. Olivas. Performance of Al-MCM-41 nano spheres as catalysts for dimethyl ether production. Catal. Today. 2022; 388: 55-62.
[20]. M. Popova, Á. Szegedi, P. Németh, N. Kostova, T. Tsoncheva, Titanium modified MCM-41 as a catalyst for toluene oxidation, Catal. Commun. 2008; 10: 304–308.
[21]. H. Song, J. Wang, Z. Wang, H. Song, F. Li, Z. Jin, Effect of titanium content on dibenzothiophene HDS Performance over Ni2P/Ti-MCM- 41catalyst. J. Catal. 2014; 311:257- 265.
[22]. Salam MS, Betiha MA, Shaban SA, Elsabagh AM, Abd El-Aal RM. Synthesis and characterization of MCM-41- Supported nano zirconia catalysts. Egypt. J. Pet. 2015; 24(1):49-57.
[23]. S. Wang, C. Ma, Y. Shi, X. Ma, Ti incorporation in MCM-41 mesoporous molecular sieves using hydrothermal synthesis. Front. Chem. Sci. Eng.2014; 8: 95–103.
[24]. N.E .Poh, H.Nur, M.N.Muhid, H. Hamdan, Sulphated AlMCM-41: Mesoporous solid Brønsted acid catalyst for dibenzoylation of biphenyl. Catal. Today. 2006; 114 (2-3): 257- 262.

.

Balakrishna Matkala, et. al. "Sulphonated Ti-MCM41: A Potential Catalyst for the Transformation of Bio-Glycerol to Solketal." *IOSR Journal of Applied Chemistry (IOSR-JAC)*, 16(1), (2023): pp 01-10.